THE ASTROPHYSICAL JOURNAL, 560:689–697, 2001 October 20

CHANDRA OBSERVATIONS AND THE NATURE OF THE ANOMALOUS ARMS OF NGC 4258 (M106)

A. S. WILSON[1] AND Y. YANG
Astronomy Department, University of Maryland, College Park, MD 20742; wilson@astro.umd.edu, yyang@astro.umd.edu
AND
G. CECIL
Department of Physics and Astronomy, University of North Carolina, CB 3255, Chapel Hill, NC 27599-3255; cecil@physics.unc.edu
Received 2001 March 6; accepted 2001 June 19

ABSTRACT

This paper presents high-resolution X-ray observations with *Chandra* of NGC 4258 and infers the nature of the so-called "anomalous arms" in this galaxy. The anomalous arms dominate the X-ray image; diffuse X-ray emission from the "plateau" regions, seen in radio and Hα imaging, is also found. X-ray spectra have been obtained at various locations along the anomalous arms and are well described by thermal (MEKAL) models with kT in the range 0.37–0.6 keV. The previously known kiloparsec-scale radio jets are surrounded by cocoons of hot X-ray emitting gas for the first 350 pc of their length. The radio jets, seen in previous VLBA and VLA observations, propagate perpendicular to the compact nuclear gas disk (imaged in water vapor maser emission). The angle between the jets and the rotation axis of the galactic disk is 60°. The jets shock the normal interstellar gas along the first 350 pc of their length, causing the hot, X-ray emitting cocoons noted above. At a height of $z = 175$ pc from the disk plane, the jets exit the normal gas disk and then propagate though the low-density halo until they reach "hot spots" (at 870 pc and 1.7 kpc from the nucleus), which are seen in radio, optical line, and X-ray emission. These jets must drive mass motions into the low-density halo gas. This high-velocity halo gas impacts on the dense galactic gas disk and shock heats it along and around a "line of damage," which is the projection of the jets onto the galactic gas disk as viewed down the galaxy disk rotation axis. However, because NGC 4258 is highly inclined ($i = 64°$), the line of damage projects on the sky in a different direction from the jets themselves. We calculate the expected P.A. of the line of damage on the sky and find that it coincides with the anomalous arms to within 2°. It is therefore proposed that the anomalous arms, which are known to lie in the galactic disk, represent disk gas that has been shocked by mass motions driven by the out-of-plane radio jets. In the inner (<1 kpc from the nucleus) regions of the galactic gas disk, the disk gas is sufficiently dense and tightly bound that it is heated to X-ray emitting temperatures, but not blown out of the disk. Thus, in this inner region, the anomalous arms are straight. Farther away from the nucleus (>1 kpc), some of the disk gas is blown out of the disk plane toward the halo on the opposite side of the disk from the relevant radio jet; this effect causes the arms to curve and is also responsible for the so-called "plateau" emission. An alternative is that the jet directions were different in the past, so they projected onto the disk in different directions. Our picture accounts for: (1) the diffuse character of the anomalous arms, (2) the inferred ionization of the optical line-emitting gas by shock waves, (3) the angle between the anomalous arms and the radio jets, (4) the sharp brightness gradients along the outer edges of the anomalous arms (these edges represent the standing shock where the high velocity, jet-driven halo gas meets the disk), (5) the existence of the plateaus, and (6) the wide range of radial velocities observed in the plateaus.

Subject headings: galaxies: active — galaxies: individual (NGC 4258) — galaxies: jets — galaxies: nuclei — galaxies: Seyfert — X-rays: galaxies

1. INTRODUCTION

The "anomalous arms" of NGC 4258 were discovered through Hα imaging by Courtès & Cruvellier (1961). These authors noted their unusual diffuse and amorphous appearance, which contrasts strongly with the knotty structure (from H II regions ionized by hot stars) of normal spiral arms. Later radio imaging by van der Kruit, Oort, & Mathewson (1972) showed that the arms are strong radio emitters, and these authors suggested that the arms are somehow powered by ejection from the galactic nucleus. Since these early works, numerous optical (e.g., Burbidge, Burbidge, & Prendergast 1963; van der Kruit 1974; Ford et al. 1986; Martin et al. 1989; Dettmar & Koribalski 1990; Rubin & Graham 1990; Cecil, Wilson, & Tully 1992, hereafter CWT; Cecil, Morse, & Veilleux 1995a; Cecil et al. 2000, hereafter C2000) and radio (e.g., van Albada & van der Hulst 1982; Hummel, Krause, & Lesch 1989; C2000; Hyman et al. 2001) studies have been made of the anomalous arms.

X-ray emission from the southeast anomalous arm was discovered by the *Einstein* HRI (CWT). NGC 4258 was imaged with both the PSPC (Pietsch et al. 1994) and the HRI (Cecil, Wilson, & De Pree 1995b, hereafter CWP) aboard *ROSAT* (see also Vogler & Pietsch 1999). The anomalous arms dominate the HRI image, although more diffusely spread X-ray emission is also detected. The PSPC spectra suggest that the X-ray emission of the anomalous arms has a thermal origin with $kT \simeq 0.3$ keV. X-ray observations with *ASCA* and *BeppoSax* have revealed a hard, heavily absorbed, power-law component that coincides

[1] Adjunct Astronomer, Space Telescope Science Institute, 3700 San Martin Drive, Baltimore, MD 21218; awilson@stsci.edu.

with the galactic nucleus, as well as the extended, softer thermal emission (Makishima et al. 1994; Reynolds, Nowak, & Maloney 2000; Fiore et al. 2001).

There is strong evidence that the anomalous arms lie in the disk of NGC 4258 (e.g., van der Kruit 1974; van Albada & van der Hulst 1982; Hummel, Krause, & Lesch 1989; Plante et al. 1991; CWT), as follows. (1) The anomalous arms extend exactly to the edge of the H I 21 cm distribution. (2) Gaps in H I 21 cm emission are observed at the positions of the principal anomalous arms. (3) The mean velocity of ionized gas along the midline of the southeast anomalous arm tends to track that of the adjacent disk. (4) If the anomalous arms were out of the plane, one would expect to see a large rotation measure from the arm on the far side of the disk, due to Faraday rotation by magnetized gas in the plane of the disk. This is not the case. Instead, the rotation measure increases in the same way when going inward along both anomalous arms. (5) In some parts of the arms, the Hα emission seems to originate from a channel or tunnel between elongated molecular clouds seen strongly in CO emission. These molecular clouds must, of course, lie in the disk. (6) Finally, the densities required for the thermal emission in both optical emission lines and X-rays are much too high for the halo of the galaxy. We thus assume that the anomalous arms are in the disk plane of NGC 4258.

Many models, all involving ejection from the nucleus in some form or other, were proposed for the anomalous arms in the 1970s and 1980s (e.g., van der Kruit et al. 1972; van Albada 1978; Icke 1979; Sofue 1980; Sanders 1982). Models with the arms out of the disk plane (e.g., Sofue 1980; Sanders 1982) can be excluded in view of their conflict with the observational data. More recently, most authors have argued that the arms represent jets emitted into the galactic disk (e.g., Ford et al. 1986; Martin et al. 1989; CWT). Discoveries in the last few years confirm that the nucleus of NGC 4258 is active and emits radio jets. These discoveries include: (1) a nuclear accretion disk (seen in water vapor maser emission) of radius $\simeq 0.3$ pc in Keplerian rotation about a putative black hole of mass $3.9 \times 10^7\ M_\odot$ (Miyoshi et al. 1995; Herrnstein et al. 1999); (2) elongated radio continuum emission on 0.01–3 pc scales that aligns closely with both the rotation axis of the accretion disk and the jetlike radio emission seen on the kiloparsec scale in VLA maps (Herrnstein et al. 1997; C2000); and (3) Mach disk and bow shock structures (seen in radio continuum and optical emission lines) that represent the ends of the currently active jets and are located 870 pc south and 1.7 kpc north of the nucleus (C2000).

However, models in which the arms represent jets or plasmoids ejected *into the disk* have serious problems. First, the radio jets are in a different direction (on the sky) from the inner anomalous arms observed in Hα and X-rays (§ 3.2). Second, models in which the jets are emitted into the galactic disk have very large energy requirements, since much dense interstellar gas must be pushed aside (cf. van Albada & van der Hulst 1982). Third, and most important, it is very difficult to see how such jets could be confined to a thin galactic gas disk while propagating to the observed distances of $\simeq 8$ kpc (4′) from the nucleus.

Previous X-ray observations (described above) have limited spectral and spatial resolutions, which have precluded a detailed study of the X-ray emission from the anomalous arms. The *ROSAT* HRI images have a resolution of $\simeq 5''$ (FWHM) but virtually no spectral resolution, while the *ROSAT* PSPC data have worse spatial resolution (25″–50″) and limited spectral resolution. The *ASCA* observations have arcminute spatial resolution and spectral resolution characteristic of CCD detectors ($\sim$100–150 eV). The *Chandra* X-ray Observatory provides subarcsecond spatial resolution and thus allows the anomalous arms to be investigated at a resolution similar to VLA radio and ground-based optical studies. The spectral resolution from direct imaging with the CCDs is similar to that attained with *ASCA*.

In this paper, we present a first observation of NGC 4258 with *Chandra*. Although the exposure time is short ($\simeq$14.0 ks), the data allow a detailed comparison between the X-rays and arcsecond resolution optical and radio images, and a crude investigation of the variation of the X-ray spectrum along the anomalous arms. We also infer the nature of the anomalous arms and show how they are related to the jets seen at radio wavelengths. We assume a distance of 7.2 Mpc (Herrnstein et al. 1999) to NGC 4258, so $1'' = 35$ pc, and adopt a Galactic hydrogen column toward NGC 4258 of $N_{\rm H}({\rm Gal}) = 1.19 \times 10^{20}\ {\rm cm}^{-2}$ (Murphy et al. 1996).

Section 2 describes the *Chandra* observations and their reduction, while § 3 presents the results of these observations. In § 4, we show that the anomalous arms represent gas in the galactic disk that has been shocked by the out-of-disk radio jets. Section 5 gives concluding remarks.

2. *CHANDRA* X-RAY OBSERVATIONS AND REDUCTION

NGC 4258 was observed with the *Chandra X-Ray Observatory* on 2000 April 17 using the Advanced CCD Imaging Spectrometer (ACIS) spectroscopic array, which provides excellent spatial resolution ($\leq 1''$) with medium spectroscopic resolution ($\simeq$130 eV FWHM at 1 keV). The default frame time of 3.2 s was used. The nucleus was centered 20″ in the $-Y$ direction from the location of best focus on chip S3. The data were inspected for background flares and times of bad aspect, but none was found. A new level 2 events file was made from the events file supplied by the *Chandra* Science Center. Response matrix files and ancillary response files were made using calibration data taken with the chip at -120 C, the temperature at the time the observations were made. The total useful integration time after all filtering was 14.0 ks. Data were analyzed using version 1.1.5 of the CIAO software and version 11.0 of XSPEC.

In the presence of large-scale X-ray emission, it is difficult to determine the level of the background. We therefore used a compilation of observations of relatively blank fields, from which discrete sources have been excised. For a particular source extraction region, a corresponding background region is taken from this compilation. The two regions have the same physical location on the S3 chip. The background images and software[2] of Maxim Markevitch were used for this procedure. The background is very low, with most pixels having zero counts.

3. RESULTS OF X-RAY OBSERVATIONS

3.1. *The Nucleus*

The region around the nucleus of NGC 4258 is shown in Figure 1. Two compact sources, separated by 2.″5 (87 pc), are apparent. The position (J2000) of the stronger source to the northeast is $\alpha = 12^{\rm h}18^{\rm m}57\overset{\rm s}{.}50$, $\delta = +47^\circ 18' 14\overset{''}{.}2$. This position coincides with both the radio continuum nucleus

[2] Available at http://hea-www.harvard.edu/~maxim/axaf/acisbg/.

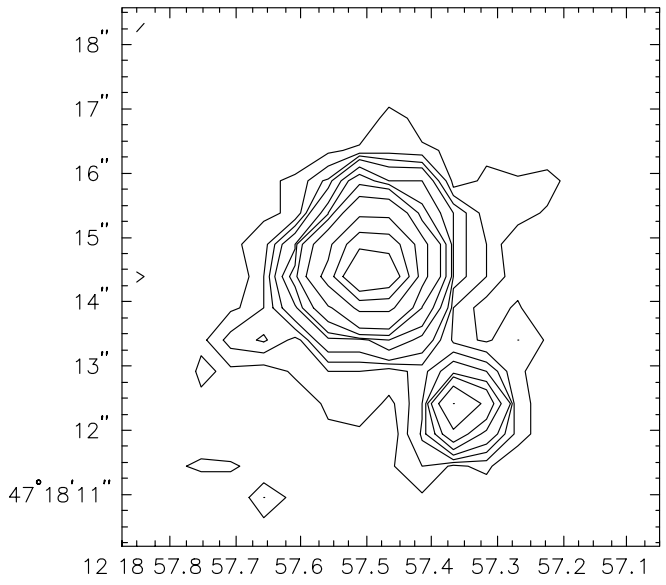

FIG. 1.—Contour map of the nucleus of NGC 4258 and its companion in the 0.3–10 keV band at the full *Chandra* resolution. Contours are plotted at 2.5, 5, 7.5, 10, 15, 20, 30, 50, 100, 200, and 300 counts pixel^{-1}.

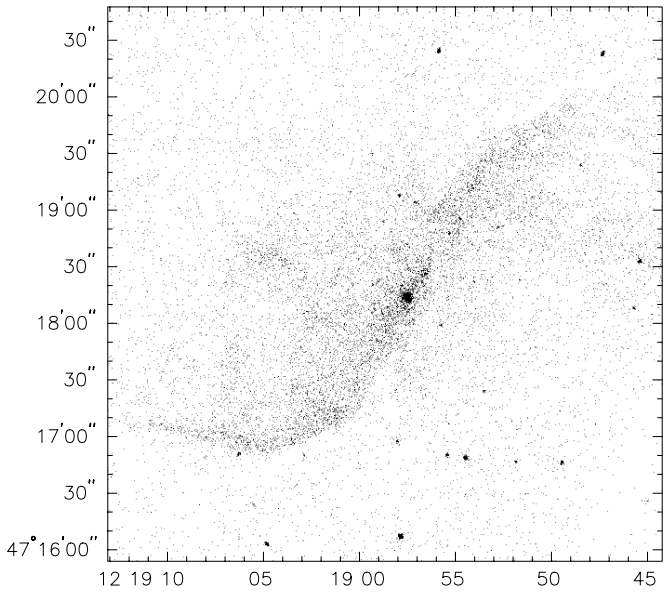

FIG. 2.—Gray-scale representation of NGC 4258 in the 0.3–8 keV band at the full *Chandra* resolution ($\lesssim 1''$).

(as measured from the $\lambda 20$ cm $1''.3$ resolution radio continuum map of C2000: $\alpha_{rc} = 12^h18^m57^s.515$, $\delta_{rc} = +47°18'14''.36$ [J2000]) and the nuclear H_2O maser source ($\alpha_m = 12^h18^m57^s.510 \pm 0^s.004$, $\delta_m = +47°18'14''.27 \pm 0''.03$ [J2000]; Greenhill et al. 1995). The nuclear source exhibits a hard spectrum with a large absorbing column density. Unfortunately, its spectrum is significantly piled-up in the present observation, which prevents us from obtaining reliable spectral parameters; an observation with a shorter frame time is planned to obtain a reliable nuclear spectrum. The spectrum of the weaker source to the southwest is well described (reduced $\chi^2 = 0.91$ for 5 degrees of freedom [dof]) by an absorbed power law spectrum, with absorbing column $N_H = 2.0^{+1.2}_{-1.1} \times 10^{21}$ cm^{-2} and a photon index $\Gamma = 1.49^{+0.50}_{-0.37}$ (the errors are 90% confidence for a single interesting parameter). The observed 0.5–4.5 keV flux is 7.0×10^{-14} erg cm^{-2} s^{-1}, and the absorption-corrected luminosity is 5.1×10^{38} ergs s^{-1} if it is associated with NGC 4258, as is very likely, given its location. The hard spectrum and X-ray luminosity suggest that the object is an X-ray binary. Most of the observed absorption is intrinsic to NGC 4258.

3.2. *The Anomalous Arms*

Figure 2 shows a gray-scale representation of the *Chandra* full-resolution image of NGC 4258. The anomalous arms are seen as diffuse structures extending to the southeast and northwest of the nucleus. The diffuse emission is better seen in Figure 3, in which the *Chandra* image has been smoothed to a resolution of $2''.7$ FWHM. X-ray emission is seen from the fainter radio-emitting regions (called "plateaus" by van der Kruit, Oort, & Mathewson 1972) to the northeast of the southeast arm and to the southwest of the northwest arm. Also apparent in the X-ray image is the bifurcation of the northwest arm $\simeq 1'$ from the nucleus, with the main arm continuing to the northwest and a weaker one extending almost due west.

Figure 4 shows the relationship between the radio and X-ray structures, both images having a resolution of $2''.7$ FWHM. The correspondence is particularly good in the outer parts of each arm more than $1'$ (2 kpc) from the nucleus. The southwest and south edges of the southeast arm and the northeast and north edges of the northwest arm are sharp in both radio and X-ray emission. An enlargement of the central region is shown in Figure 5. In the first $7''$–$10''$ (250–350 pc) of the jet to the north, the X-rays are seen to exhibit a "two-pronged" structure, enveloping the radio jet. This morphology suggests that the X-rays originate in a hot cocoon around the high-velocity material responsible for the radio emission. Within $1'$ (2 kpc) of the nucleus, the brightest X-ray emission is aligned in P.A. $\simeq -33°/147°$, in excellent agreement with the P.A. $\simeq -30°/150°$ of the Hα arms, but in contrast to the almost north-south alignment of the radio emission. Taken

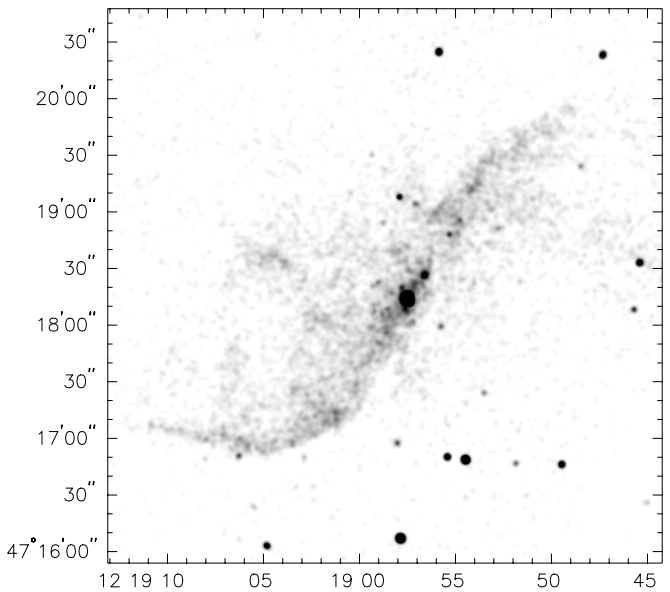

FIG. 3.—Gray-scale representation of NGC 4258 in the 0.3–8 keV band with a resolution of $2''.7$ (FWHM).

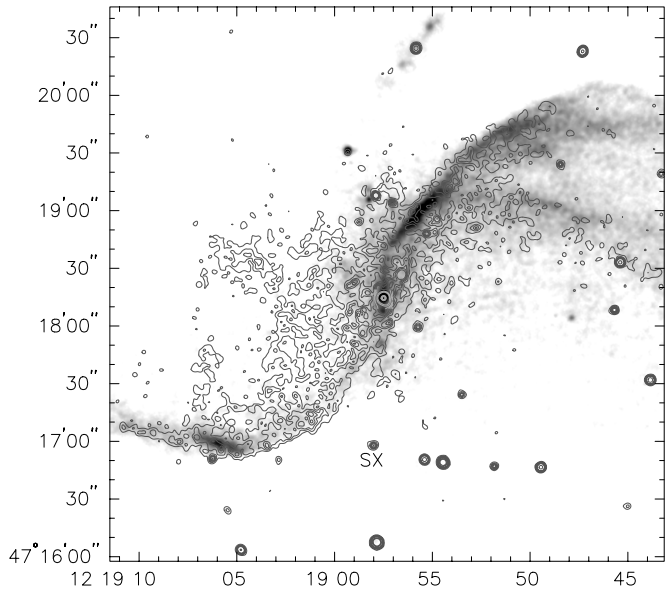

FIG. 4.—Superposition of radio (*gray scale*) and X-ray (*contours*) images of NGC 4258. The radio image is at 1.49 GHz and was obtained with the VLA by Cecil et al. (2000). Both images have a resolution of 2.″7 (FWHM). Contours of the *Chandra* image are plotted at 3, 6, 9, 12, 15, 20, 50, 100, 500, 1000, and 1500 counts pixel^{-1}. The compact X-ray source 77″ south of the nucleus, which aligns with the nucleus and north radio hot spot, is marked by "SX" (§ 3.2).

together with the close alignment between radio and X-ray emission farther out, the net effect is that the X-ray arms appear straighter than the radio arms in lower resolution X-ray images (CWP; Vogler & Pietsch 1999). The "north radio hot spot" (marked as "N" in Fig. 5) is located 49.″9 (1.7 kpc) north (P.A. $-5°$) of the nucleus. C2000 identified this feature as the end of the currently active jet in view of (1) its association with features suggestive of an oblique bow shock and Mach disk in a *Hubble Space Telescope* (*HST*) Hα + [N II] λ6583 image, and (2) the detailed kinematics of high-velocity gas in long-slit spectra at this location. Close to the north radio hot spot, there is a compact X-ray source with a sharp "leading" edge (i.e., to the north) and a slower brightness decline on the upstream side (to the south; see Fig. 5). In the full-resolution *Chandra* image, this source is elongated by $\simeq 3''$ in a northeast-southwest direction, much like the Hα + [N II] and radio brightness distributions in the *HST* and full-resolution VLA images, respectively. This morphology is suggestive of thermal X-ray emission from post–bow-shock or entrained jet gas, and supports the idea that these radio, optical, and X-ray features mark the head of the currently active northern jet. A corresponding, but weaker, feature (the "south radio hot spot," marked "S" in Fig. 5) is found in the radio map 24.″5 (860 pc) south (P.A. 178°) of the nucleus. The south radio hot spot itself is not detected in X-rays, but there is a weak (two contours in Fig. 5) enhancement of the X-ray emission 3″ ahead (south) of the radio emission, which might represent gas heated by the bow shock. This X-ray enhancement seems also to be ahead of the bowlike optical line emission (visible at the bottom of Fig. 7), consistent with the latter being postshock cooled gas. Farther along this same direction, a compact X-ray source is found 77″ (2.7 kpc) south (P.A. 176°) of the nucleus (marked as "SX" in Fig. 4). The position (J2000.0) of this source is $\alpha = 12^{h}18^{m}58^{s}.02$, $\delta = +47°16'57''.5$. No radio source is detected at this location. This X-ray source, the nucleus, and the north radio hot spot align to within $\simeq 1°$. It is tempting to speculate that this source may represent another jet-ISM interaction, but there is no evidence, other than the alignment, that this X-ray source is associated with NGC 4258.

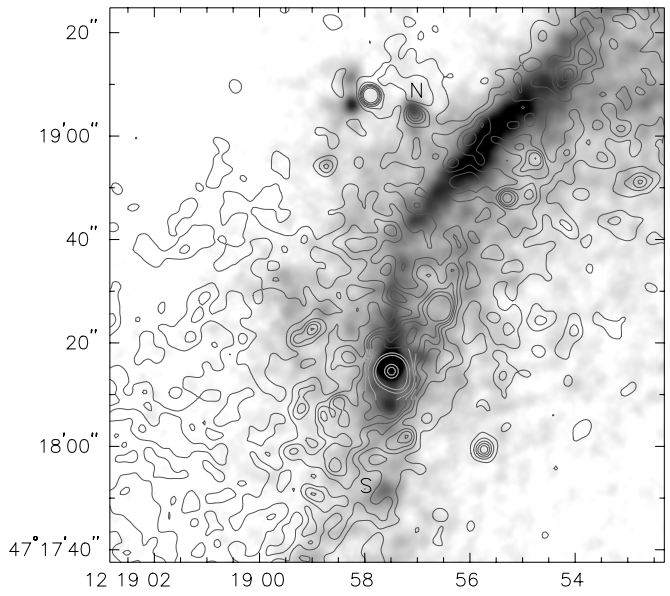

FIG. 5.—Superposition of radio (*gray scale*) and X-ray (*contours*) images in the inner regions of NGC 4258. The radio map and the X-ray contours are as in Fig. 4. The north and south radio hot spots are indicated by "N" and "S," respectively.

Figure 6 compares the large-scale X-ray and Hα distributions of NGC 4258. With the exception of a number of point sources, the normal spiral arms are not seen in X-rays. There is an excellent overall correspondence between the X-ray and Hα emissions of the anomalous arms. In particular, the X-ray and Hα emissions align within 1′ of the nucleus, where the radio jet follows a different (almost north-south) direction, as already noted.

Figure 7 is a superposition of X-ray contours on an *HST* Hα + [N II] λ6583 image (from C2000) of the inner regions of NGC 4258. Both images are dominated by the diffuse emission of the anomalous arms. It is notable that the first 5″–6″ (175–210 pc) of the "two-pronged" X-ray structure to the north of the nucleus (Fig. 5) aligns with two radial Hα + [N II] filaments. These filaments form the inner part of what C2000 termed a "nuclear loop" (see Fig. 5 of C2000)—a roughly circular, line-emitting structure open to the north.

We have investigated the variation of the spectrum of the X-ray emission along the anomalous arms. A spectrum was obtained for each of nine regions along the arms. All regions show soft X-rays, but the inner regions exhibit, in addition, a hard X-ray component above 3 keV. Examination of an image in the 3–8 keV band shows that the emission is circularly symmetric and centered on the nucleus. We have compared the radial distribution of this emission with that expected from the telescope point-spread function (PSF) and found good agreement. It is thus clear that this extended hard emission is not real but results from scattering of nuclear X-rays by the *Chandra* mirrors. We therefore restricted our spectral modeling to the 0.3–2.0 keV band to avoid contamination by this hard component.

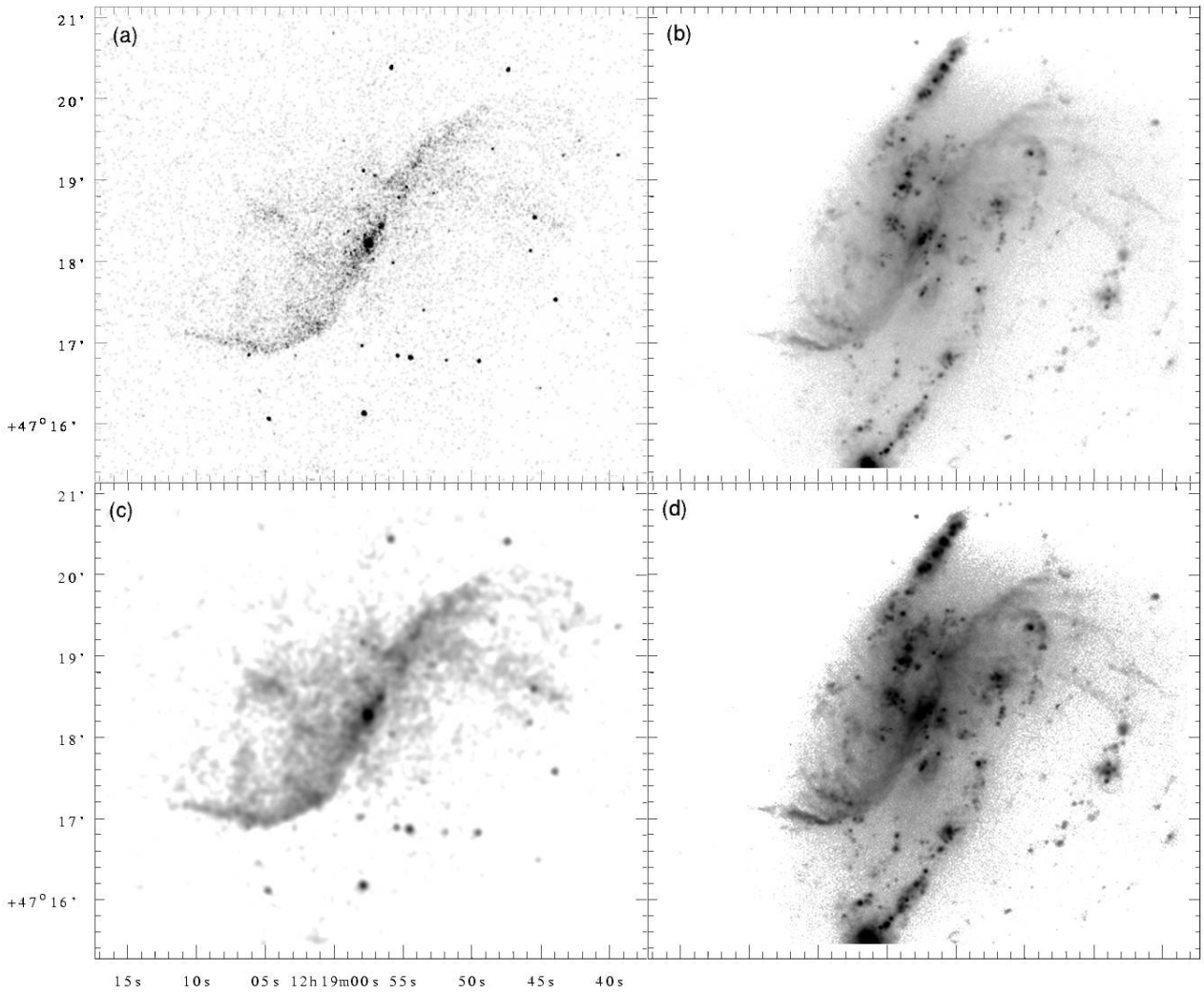

FIG. 6.—Comparison of X-ray (*left*) and Hα (*right*; from C2000) images of NGC 4258. The top left panel shows the full-resolution *Chandra* image, while the bottom left shows the image convolved to 2.″7 FWHM. The two Hα images (*top and bottom right*) are identical but displayed with different contrasts. The FWHM resolution of the Hα images is $\simeq 1''$ (C2000).

Each region was modeled by a single absorbed MEKAL plasma, with the abundance and absorbing column allowed to vary. This model provides an approximate description of the spectra (χ^2/dof ranges from <1 to 1.7). The details of the fits are not believable, but they indicate temperatures kT in the range 0.37–0.6 keV with no apparent trend with distance from the nucleus. At the ends of the arms, the required column density is consistent with the Galactic column, but farther in there appears to be absorption intrinsic to NGC 4258. An example of the spectra is shown in Figure 8. This represents a rectangular region centered 64″ southeast of the nucleus with long dimension (along the arm) 38″ and short dimension 26″. Details of the model are given in the figure caption. A more detailed discussion of the X-ray spectra of the arms is deferred until a longer *Chandra* integration, scheduled for cycle 2, has been obtained.

4. THE NATURE OF THE ANOMALOUS ARMS

4.1. *The Radio Jets*

The north and south radio hot spots, located 1.7 kpc and 870 pc, respectively, from the nucleus align closely with all of: (1) the radio jet extending $\simeq 700$ pc north and $\simeq 400$ pc south of the nucleus (cf. Fig. 5); (2) the radio continuum features seen with VLBI, which extend 0.01–0.07 pc from the center of the maser disk (presumed to be the location of the black hole); and (3) the projection of the rotation axis of the maser disk on the sky. In particular, the north and south hot spots lie in P.A. $-5°$ and 178°, respectively, within 6° of the projected inner disk rotation axis of $-8°/172°$ reported by Herrnstein et al. (1999). We conclude that the maser disk has not changed its axis significantly over the time the jets have taken to reach the hot spots. Given that the north radio hot spot is 1.7 kpc from the nucleus, the corresponding jet material left the nucleus at least $5.1 \times 10^{21}/c$ s = 5700 yr ago. If the disk is precessing, the above noted alignment then implies a precessional period of $\geq 3 \times 10^5$ yr. This number was obtained by assuming that any tilt of the inner regions of the disk over the last 5700 yr is less than 6°, i.e., this time is 1/60 of a precessional period.

We now define the direction of the jet in three dimensions. Following the nomenclature of Clarke, Kinney, & Pringle (1998; see their Fig. 1), let ϕ be the angle between the jet and our line of sight, δ be the angle between the projection of the jet onto the plane of the sky and the apparent major axis of the galaxy disk (also in the plane of the sky), i be the inclination of the galaxy disk, and β be the angle between the jet and the galaxy disk rotation axis. The

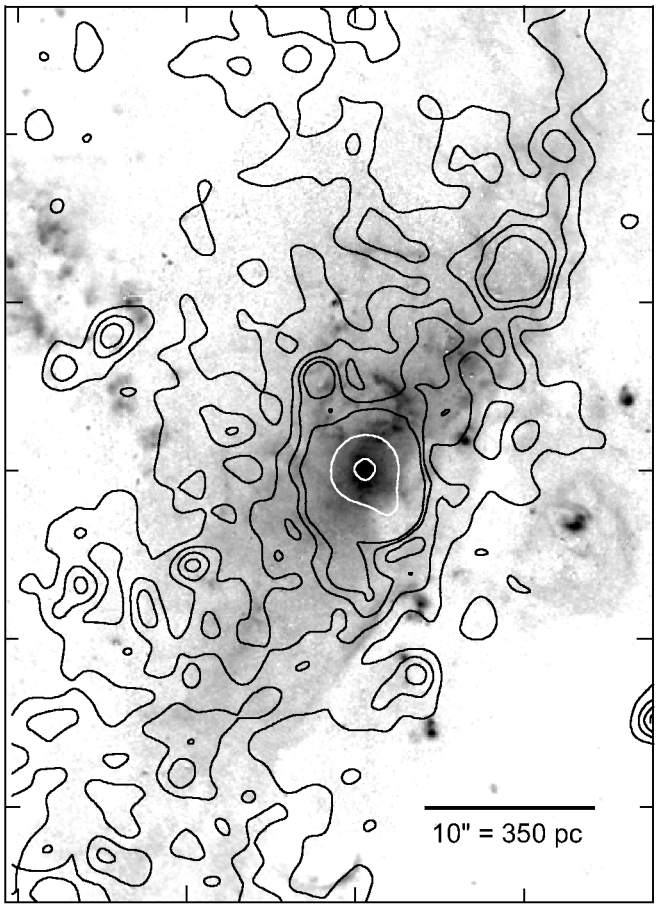

FIG. 7.—Superposition of the X-ray image with resolution FWHM = 2.″0 (*contours*) on an *HST* image in the light of Hα + [N II] λ6583 (from C2000). Contours are plotted at 3, 6, 9, 12, 120, and 1200 counts pixel^{-1}. North is up and east to the left. The ticks on the border are separated by 10″. The correspondence between the "two-pronged" X-ray emission extending 5″–6″ north of the nucleus and the Hα + [N II] emission of the "nuclear loop" is notable (see text).

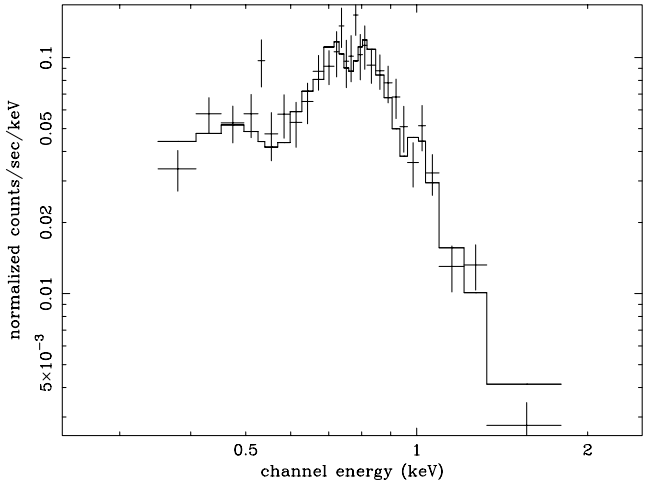

FIG. 8.—Spectrum of a region, described in the text, along the anomalous arm to the southeast of the nucleus. The model, shown as the histogram, is a MEKAL with the column density N_H, temperature, T, abundance, and normalization, K, as free parameters. The model has $N_H = 2.8^{+8.2}_{-2.8} \times 10^{20}$ cm^{-2} (and is thus consistent with the Galactic column), $kT = 0.48^{+0.05}_{-0.12}$, abundance $0.12^{+0.05}_{-0.06}$, and $K = 3.09^{+5.22}_{-1.07} \times 10^{-4}$. Errors are 90% confidence for a single interesting parameter. The parameter K is defined as $10^{-14} \int n_e n_H dV / \{4\pi[(1+z)D_A]^2\}$, where n_e is the electron density (cm^{-3}), n_H is the hydrogen density (cm^{-3}), V is the volume (cm^3), z the redshift, and D_A is the angular size distance to the source (cm).

angle ϕ is presumably equal to the inclination of the maser disk, given as 82° by Herrnstein et al. (1999). The P.A. of the jet on the sky is −5°, and the P.A. of the major axis of the galaxy disk is 146° (CWT), so the angle between them $\delta = 29°$. The inclination of the galaxy disk is $i = 64°$ (e.g., CWT). The angle β is given by

$$\cos\beta = \sin\delta \sin i \sin\phi + \cos i \cos\phi , \qquad (1)$$

so $\beta = 60°$, in agreement with C2000. The north jet is tilted slightly toward us and the south jet slightly away. The northeast side is the far side of the galaxy disk and the southwest side the near, based on both the sense of curvature of the normal spiral arms plus the observed rotation sense of the galaxy, and the pattern of dust obscuration. Thus the north (south) radio jet is on the near (far) side of the galaxy disk (see Fig. 9).

The "two-pronged" structure of the X-ray emission enveloping the jet extends ≃250−350 pc from the nucleus to the north (§ 3.2, Fig. 5). After this, the X-ray intensity decreases sharply. A weaker, not obviously two-pronged, feature extends a similar distance south. As noted above, we believe that these X-rays originate in a hot, shocked cocoon surrounding the jet. This interpretation is consistent with the Hα + [N II] filaments (§ 3.2, Fig. 7) associated with the two X-ray prongs to the north of the nucleus. These optical filaments form a "nuclear loop" (C2000), a roughly circular structure open on its north side and suggestive of gas in the jet-heated cocoon that has cooled to a few × 10^4 K. The Hα + [N II] emission is brighter on the western than the eastern side of the loop (see Fig. 5 of C2000 and the present Fig. 7) because the western gas is in the galaxy disk and is, presumably, denser.

Given the above-defined geometry of the jets, they are at a height $z = 170$ pc above the galactic disk when the X-ray emitting cocoons end. We argue that the X-ray emissions of the cocoons end when the jets exit the normal, dense gas disk of NGC 4258. There is only weak X-ray and Hα emission along the rest of the jets (as far as the radio hot spots) because the jets extend out of the plane of the galaxy disk ($\beta = 60°$), and the gas density at these distances ($|z| \geq 170$ pc) from the galactic disk is too low for significant thermal emission.

4.2. *The Inner Anomalous Arms*

It is notable that the northwest extension of the brightest X-rays lies in P.A. −33° and extends northwest from the northwest prong of the two-pronged structure discussed above and visible in Figures 5 and 7. This continuity strongly suggests that the X-ray and Hα anomalous arms represent gas in the disk of the galaxy that is, in some way, connected with the out-of-plane radio jets.

The out-of-plane jets presumably propagate within a low-density gas, as mentioned above. The jets must drive mass motions and shock waves into this gas, and these motions will propagate in all directions. The density out of the galaxy plane is too low for strong X-ray emission, but the high-velocity, low-density halo gas must collide with the dense gas in the galaxy disk and could heat it to X-ray emitting temperatures. This influence of the out-of-plane,

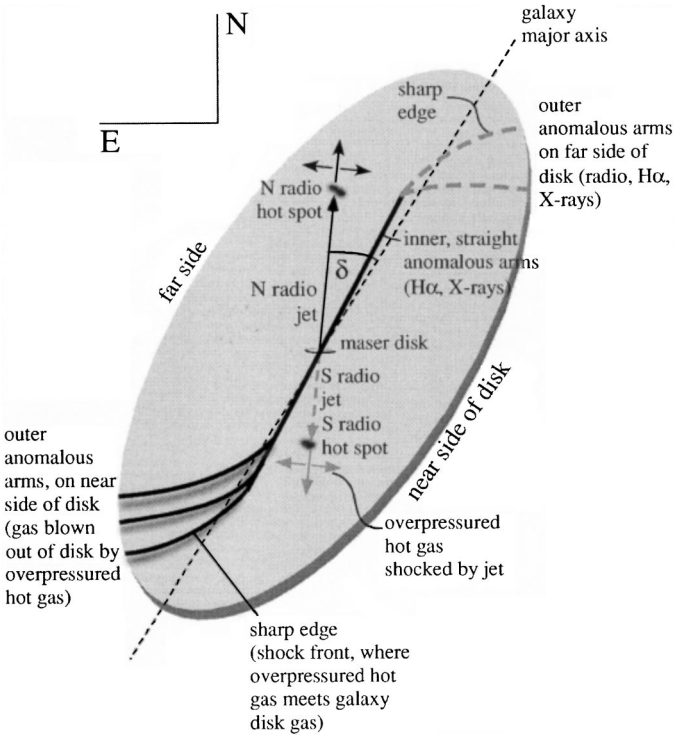

FIG. 9.—Schematic diagram (not to scale) showing the nuclear maser disk, the radio jets, the radio hot spots, the galactic disk and the anomalous arms. The north (south) radio jets are on the near (far) side of the galactic disk. We show in § 4 that the inner anomalous arms represent the projection of the jets onto the plane of the galactic disk when viewed down the rotation axis of the galactic disk. We argue that the anomalous arms represent dense disk gas that has been shocked by gas driven down onto the disk by the out-of-plane radio jets. The arms begin to curve some 1′ (2 kpc) from the nucleus because at these larger radii the gas is of lower density and less tightly bound to the galaxy. The mass motions driven by the jet can then push gas out of the disk in the opposite direction, causing the extended emission features ("plateaus") seen in radio, X-ray, and optical line emission. On the side of the anomalous arms closest to the jets, there is a shock front between the high-velocity, low-density halo gas and the dense disk gas; this shock front is seen as the sharp edges of the anomalous arms on the sides that project toward the jets. See § 4 for further details.

straight jets on the disk will be strongest along the straight line that represents the locus in the galaxy disk to which the jets are closest. This locus is just the projection of the jets onto the galaxy disk from a distant viewpoint along the rotation axis of the galaxy disk. However, from our perspective, the galaxy is highly inclined ($i = 64°$), which means that the projection of this locus on the plane of the sky is tilted with respect to the projection of the jets on the plane of the sky.

We thus need to derive the angle, α, between the projection onto the plane of the sky of the locus in the galaxy disk to which the jets are closest and the galaxy disk major axis. This locus is, of course, a straight line as long as the jet is straight and the galactic disk is not warped. In terms of the angles defined earlier,

$$\cos \alpha = \frac{\sin \phi \cos \delta}{(\sin^2 \beta \cos^2 i + \sin^2 i \sin^2 \phi \cos^2 \delta)^{1/2}} . \quad (2)$$

Substituting the values given earlier gives $\alpha = 2°.5$. Since the P.A. of the galaxy disk major axis is 146°, the predicted P.A. of the projection onto the plane of the sky of the locus in the galaxy disk to which the jet is closest is 148°.[3] *This P.A. is in excellent agreement with that of the X-ray/*Hα *emission within* 2 kpc *of the nucleus.* We therefore conclude that the straight part of the anomalous arms (within 1′ [2 kpc] of the nucleus) represents the locus in the galaxy disk to which the jets are closest. As discussed above, the "damage" done by the jets will be greatest along this line, and the anomalous arms then represent gas in the disk that has been shocked by mass motions driven by the out-of-plane jets (Fig. 9). The optical emission-line ratios indicate that the gas in the anomalous arms is, indeed, ionized by shocks (e.g., van der Kruit 1974; Dettmar & Koribalski 1990; Cecil et al. 1995a).

The diffuse character of both the X-ray (Fig. 2) and Hα (Fig. 7) arms supports the above scenario. A true jet within the galactic disk would be expected to contain narrow, bright structures at all wavelengths. In contrast, the blast wave driven into the disk by the out-of-plane jet spreads over a significant width in the disk, producing hot gas in a wide, diffuse linear structure without sharp features.

4.3. *The Outer Anomalous Arms*

The above-described situation, in which the arms lie strictly within the disk plane and represent the projection of the straight out-of-plane jets onto the disk, must break down at $>1'$ (2 kpc) from the nucleus, because here the arms are observed to curve in a clockwise sense. As long as the jets are straight and the disk is unwarped, the projection of the jets onto the disk must be a straight line. Two features of the morphologies of the outer arms seen in *all wavebands* (i.e., radio continuum, X-rays, and optical emission lines) are crucial at this point:

1. The very sharp brightness gradients seen on the outer edges of the arms (i.e., the southwest and south sides of the southeast arm and the northeast and north sides of the northwest arm). Images that show these sharp edges well include Figures 4 and 6 of the present paper, Figures 1 and 2 of van Albada & van der Hulst (1982), and Figure 6*a* of Hyman et al. (2001). It is notable that these sharp edges are on the side of the arms which projects closest to the corresponding out-of-plane radio jet.

2. The extended, diffuse emissions (plateaus) and filaments on the inner sides of the arms (i.e., the northeast and north sides of the southeast arm and the southwest and south sides of the northwest arm). Images that show these structures well include the same figures cited above, plus the Hα images shown as Figure 19 of CWT and Figures 1*a* and 1*b* of C2000. These extended, diffuse emission regions are on the *opposite* side of the arms to the corresponding out-of-plane radio jet.

Close to the center of the galaxy, the gas in the galaxy disk is dense and tightly bound gravitationally to the disk plane. Farther out, the gas density decreases and the gas is also less tightly bound. We speculate that the process of excitation of the outer anomalous arms is the same as proposed for the inner arms, namely, the impact of mass motions driven down from the galactic halo by the radio jet. The sharp edges are then naturally accounted for as shock

[3] The projection onto the plane of the sky of the projection of the jet onto the galaxy disk must lie between the projection of the jet onto the sky and the galaxy major axis. Therefore, in the solution of equation (2), α must be positive.

fronts where the fast-moving light halo gas meets the dense disk gas; as noted above, the sharp edge is on the side of the anomalous arm toward the relevant radio jet (Fig. 9). It may be that the relativistic electrons required for the radio emission of the outer anomalous arms are accelerated at these shock fronts. The arms curve because the impact is now sufficient to begin to drive gas out of the galaxy disk. The extended emission ("plateaus") and filaments represent gas that has been driven out of the gas disk toward the galaxy halo on the opposite side of the disk to the relevant radio jet (Fig. 9). This gas is shock ionized, as inferred from the optical emission-line ratios.

In this hypothesis, we expect a wide range of gas motions in the regions of diffuse emission; here, the observed Doppler motions should differ from the normal rotational motion of the galaxy at the projected location on the sky. These "anomalous velocities" should be both positive and negative with respect to normal rotation, because the gas will be driven out of the disk in a range of directions with respect to the disk normal, and the galaxy disk is highly inclined. Further, some of the gas could be falling back onto the disk, as envisaged by Rubin & Graham (1990). Such wide ranges of velocity have been observed in the diffuse emission ("plateaus") in Hα by van der Kruit (1974) and Rubin & Graham (1990) and in H I 21 cm emission by van Albada & Shane (1975). Rubin & Graham (1990) note that, in their spectrum along P.A. 125°, the range of velocities in the southeast diffuse emission is larger than that seen in the corresponding emission to the northwest. They ascribe the difference to obscuration of the diffuse emission on the northwest side of the galaxy by the intervening, near side of the galactic disk, in accord with our model (Fig. 9).

An alternative explanation for the curvature of the outer anomalous arms is that the jet directions were different in the past, so their projections onto the disk would also have been different. A progressive change of the jet axes with time (e.g., through "disk precession") would lead to curved jets with a curved projection onto the stellar disk. In such a picture, the plateaus would represent material in the galactic disk that was shocked by the out-of-plane jets in the past, when the jet directions were different.

5. CONCLUDING REMARKS

5.1. *X-Ray Results*

Our *Chandra* observations have revealed the X-ray structure of the "anomalous arms" of NGC 4258 with the highest resolution to date. The X-rays are found to envelop the inner (first 350 pc) of the northern jet, indicating that they originate from a hot, presumably shocked, cocoon. Farther out (to $\sim$2 kpc from the nucleus), the straight ridge of the brightest X-rays is rotated by $\sim$30° in a clockwise sense with respect to the radio jet. There is a very tight association between the X-ray and Hα emissions of the anomalous arms. In the outermost regions of detected X-ray emission, where the arms curve in a trailing sense with respect to galactic rotation, the X-ray and radio arms also correspond well. The spectrum of the X-rays from the anomalous arms indicates a thermal origin with temperatures in the range 0.37–0.6 keV, with no apparent trend with distance from the nucleus.

The currently active radio jets project almost north-south on the sky. Both end at well-defined radio hot spots, which are associated with structures seen in Hα + [N II] images suggestive of a Mach disk and bow shock (C2000). X-rays are detected from the north radio hot spot; the X-ray morphology reveals a sharp "leading" (i.e., to the north) edge and a slower decline on the "trailing" edge, suggestive of emission from a shock. The south radio hot spot is not detected in X-rays, but weak enhanced X-ray emission is found ahead (south) of the radio peak.

5.2. *The Anomalous Arms*

The combined radio, Hα, and X-ray images have allowed us to elucidate the nature of the anomalous arms. The radio jets in the inner $\sim$kiloparsec align perpendicular to the compact, circumnuclear gas disk, which has been imaged in water vapor maser emission. The inclination of this disk is known, so the three-dimensional orientation of the jet can be deduced. The angle between the jet and the rotation axis of the galaxy disk is then found to be $\beta = 60°$.

When the jets initially leave the nucleus, they are surrounded by the dense normal gas disk of the inner regions of this SABSbc galaxy. The jets shock this gas, producing a hot cocoon that envelops the jets and emits strongly in X-rays and optical emission lines, as noted above (see also Figs. 5 and 7). At a height of $|z| = 175$ pc from the galactic disk, the jets exit the dense galactic disk and then propagate in a low-density medium until they come to the "north radio hot spot" and the "south radio hot spot," located 1.7 kpc and 870 pc from the nucleus, respectively (Fig. 5). The existence of a compact X-ray source 77″ (2.7 kpc) south of the nucleus (Fig. 4), aligned to within 1° with the jet farther in, hints that the jets may propagate beyond the hot spots. During this phase, the jets heat, and drive mass motions into, the surrounding gas, but little X-ray emission results because of the low density of the gas in the galactic halo.

The jets, propagating supersonically at 30° to the plane of the galaxy, drive mass motions and shocks in all directions. The mass motions propagating toward the plane of the galaxy meet the dense gas disk and heat it to X-ray emitting temperatures (§ 3.2). The greatest "damage" done by the jet will be along its projection onto the galaxy gas disk, as viewed down the disk rotation axis. Since NGC 4258 is substantially inclined ($i = 64°$), however, this "line of damage" projects on the sky in a different direction to the jet itself. Because the three-dimensional geometry is fully known, we can calculate the angle between the jet and the line of damage projected onto the sky. This simple calculation shows that the anomalous arms (observed in X-rays and Hα) coincide with the expected line of damage to within 2°.

The picture that emerges is one of a bipolar jet inclined at 30° to the galactic gas disk and driving shocks into it. This scenario accounts naturally for the diffuse structure of the arms, since the shocks from the jet heat up a wide area of the disk. Preexisting molecular clouds may be too dense to be heated by these shocks, so the inner anomalous arms represent hot, lower density regions between these clouds, as observed (Martin et al. 1989; CWT). The optical line emission represents gas in the galactic disk that has been shock ionized and has then cooled (van der Kruit 1974; Dettmar & Koribalski 1990; Cecil et al. 1995a). For this reason, the X-ray and Hα distributions agree closely.

In the inner regions (<1 kpc from the nucleus) of the galaxy, the gas density is high and it is tightly bound gravitationally. The blast waves driven into the gas heat it to ≤ 1 keV, but are unable to drive the hot gas out of the disk. In

this region, the line of damage is a straight line in the disk, so the anomalous arms appear straight on the sky. Farther out (> 1 kpc from the nucleus), the gas in the disk is of lower density and less tightly bound. The impact of the low-density halo gas driven by the jet onto the disk then suffices to drive the disk gas out of the disk plane. Each arm then curves away from the radio jet that powers it. An alternative scenario for the curvature of the anomalous arms would involve changes in the jet directions over time.

In summary, this scenario accounts for:

1. The diffuse character of the anomalous arms.
2. The observation that the optical line ratios indicate ionization by shocks.
3. The angle between the radio jet and the anomalous arms.
4. The sharp brightness gradients along the outer edges of the arms; these edges are on the side of the arm nearest to the relevant radio jet. The sharp edges represent standing shocks at the interface between the low-density halo gas being driven by the jet onto the gas disk and the gas disk itself.
5. The diffuse gas and filaments (plateaus) on the opposite side of the disk to each jet. These structures, seen in optical emission lines, X-rays, and radio continuum, are gas that has been pushed out of the disk toward the halo by the impact of the low-density high-velocity halo gas driven by the jet on the other side of the disk.
6. The observed wide range of velocities of the diffuse gas and filaments.

A prediction of this model is the existence of extremely hot, high-velocity gas in the two quadrants of the galaxy halo occupied by the radio jets. X-ray absorption spectra of quasars in these quadrants could be used to search for this gas. The unique character of the anomalous arms in NGC 4258 is probably related to the presence of *both* powerful jets (generally seen only in early-type galaxies) and a dense, galactic gas disk (generally seen only in late-type galaxies). Our scenario could be evaluated quantitatively by a hydrodynamic simulation, which would allow the required parameters (e.g., jet power, halo gas density, disk gas density, etc.) to be derived.

This research was supported by NASA through grant NAG8-1027 and by the Graduate School of the University of Maryland through a research fellowship to A. S. W. We are grateful to A. J. Young for advice on the *Chandra* analysis and to Stephen M. White for a helpful discussion. We also wish to thank the staff of the *Chandra* Science Center, especially Dan Harris and Shanil Virani, for their help, and the anonymous referee for useful comments.

REFERENCES

Burbidge, E. M., Burbidge, G. R., & Prendergast, K. H. 1963, ApJ, 138, 375
Cecil, G., Greenhill, L. J., DePree, C. G., Nagar, N., Wilson, A. S., Dopita, M. A., Pérez-Fournon, I., Argon, A. L., & Moran, J. M. 2000, ApJ, 536, 675 (C2000)
Cecil, G., Morse, J. A., & Veilleux, S. 1995a, ApJ, 452, 613
Cecil, G., Wilson, A. S., & De Pree, C. 1995b, ApJ, 440, 181 (CWP)
Cecil, G., Wilson, A. S., & Tully, R. B. 1992, ApJ, 390, 365 (CWT)
Clarke, C. J., Kinney, A. L., & Pringle, J. E. 1998, ApJ, 495, 189
Courtès, G., & Cruvellier, P. 1961, Compt. Rend. Acad. Sci. Paris, 253, 218
Dettmar, R.-J., & Koribalski, B. 1990, A&A, 240, L15
Fiore, F., et al. 2001, ApJ, 556, 150
Ford, H. C., Dahari, O., Jacoby, G. H., Crane, P. C., & Ciardullo, R. 1986, ApJ, 311, L7
Greenhill, L. J., Jiang, D. R., Moran, J. M., Reid, M. J., Lo, K.-Y., & Claussen, M. J. 1995, ApJ, 440, 619
Herrnstein, J. R., et al. 1997, ApJ, 475, L17
———. 1999, Nature, 400, 539
Hummel, E., Krause, M., & Lesch, H. 1989, A&A, 211, 266
Hyman, S. D., Calle, D., Weiler, K. W., Lacey, C. K., van Dyk, S. D., & Sramek, R. 2001, ApJ, submitted
Icke, V. 1979, A&A, 74, 42
Makishima, K., et al. 1994, PASJ, 46, L77
Martin, P., Roy, J.-R., Noreau, L., & Lo, K. Y. 1989, ApJ, 345, 707
Miyoshi, M., et al. 1995, Nature, 373, 127
Murphy, E. M., Lockman, F. J., Laor, A., & Elvis, M. 1996, ApJS, 105, 369
Pietsch, W., Vogler, A., Kahabka, P., Jain, A., & Klein, U. 1994, A&A, 284, 386
Plante, R., Lo, K.-Y., Roy, J.-R., Martin, P., & Noreau, L. 1991, ApJ, 381, 110
Reynolds, C. S., Nowak, M. A., & Maloney, P. R. 2000, ApJ, 540, 143
Rubin, V. C., & Graham, J. A. 1990, ApJ, 362, L5
Sanders, R. H. 1982, in IAU Symp. 97, Extragalactic Radio Sources, ed. D. S. Heeschen & C. M. Wade (Dordrecht: Reidel), 145
Sofue, Y. 1980, PASJ, 32, 79
van Albada, G. D. 1978, Ph.D. thesis, Univ. of Leiden
van Albada, G. D., & Shane, W. W. 1975, A&A, 42, 433
van Albada, G. D., & van der Hulst, J. M. 1982, A&A, 115, 263
van der Kruit, P. C. 1974, ApJ, 192, 1
van der Kruit, P. C., Oort, J. H., & Mathewson, D. S. 1972, A&A, 21, 169
Vogler, A., & Pietsch, W. 1999, A&A, 352, 64